

Article

Spectroscopy and 1 μ m Luminescence by Visible Quantum Cutting in Pr³⁺-Yb³⁺ Codoped Glass

Yumiko Katayama * and Setsuhisa Tanabe

Graduate School of Human and Environmental Studies, Kyoto university / Yoshida-nihonmatsu-cho, Sakyo-ku, Kyoto 606-8501, Japan; E-Mail: stanabe@gls.mbox.media.kyoto-u.ac.jp (S.T.)

* Author to whom correspondence should be addressed;

E-Mail: yumiko@h05ktym.mbox.media.kyoto-u.ac.jp; Tel.: +81-75-753-6817;

Fax: +81-75-753-6694.

Received: 28 December 2009; in revised form: 25 January 2010 / Accepted: 25 March 2010 /

Published: 29 March 2010

Abstract: The quantum cutting phenomenon of a blue photon into two infrared photons is reported in glass codoped with Pr³⁺-Yb³⁺ ions. Oxyfluoride glass with compositions of 32SrF₂-0.1PrF₃-2.9YbF₃-42SiO₂-23Al₂O₃ were prepared, and photoluminescence properties in the range from visible to near-infrared were investigated. Evidence of several energy transfers, such as (Pr³⁺:³P₀→¹G₄)→(Yb³⁺:²F_{5/2}←²F_{7/2}) and (Pr³⁺:¹D₂→³F₄, ³F₃)→(Yb³⁺:²F_{5/2}←²F_{7/2}), were demonstrated in the Pr³⁺-Yb³⁺ co-doped glass. By comparing excitation spectrum of the Yb³⁺ emission with absorption spectrum of Pr³⁺, we obtain direct evidence of quantum cutting by excitation to Pr³⁺:³P_J levels at 420 ~ 490 nm.

Keywords: quantum cutting; praseodymium; ytterbium; glass; solar energy

1. Introduction

The quantum cutting (QC) phosphors that convert a photon into two photons with lower energy have been studied because of their application for such purposes as in fluorescent tubes, plasma display panels and solar cells. In 1974, it was reported that a phosphor doped with Pr³⁺ ions showed QC, which converted a vacuum ultra violet (VUV) photon into 400 nm (¹S₀→¹I₆, ³P_J) and 480 nm (³P₀→³H₄) visible photons [1,2]. Since this report, phosphors that show QC from VUV to visible lights have been reported in materials doped with several rare earth ions and rare earth ions pairs, such as Pr³⁺ [1,2], Gd³⁺ [3],

Gd³⁺-Eu³⁺ [4]. These phosphors have been studied as a replacement for the Hg discharge and high quantum efficiency phosphors.

Recently, rare earth ions pairs, RE³⁺-Yb³⁺ (RE = Pr, Tb, Tm) that show visible to near-infrared QC have been reported [5–8]. These materials have attracted a great attention because they have potential to enhance efficiency of crystalline silicon (c-Si) solar cells [9–11]. The solar cells, which are generally based on photovoltaic effect of semiconductor, can obtain electricity from photons that have energy equal to or higher than the bandgap. However, in the case of higher-energy photons, the excess energy of incident photons is changed into heat. This thermal loss is one of the major reasons that photoelectric conversion efficiency of a single-junction solar cell, even with optimum bandgap for the solar spectrum, is limited up to 29% [12]. Among the various solar cells ever developed, the c-Si cell is most widely used because of its many practical advantages. Therefore, it has been reported that spectral modification of the solar spectrum is one solution for further improvement of the conversion efficiency. Since the Yb³⁺:²F_{5/2}→²F_{7/2} emission and sensitivity peak of silicon solar cell overlap each other, these QC materials, which convert a photon in the UV to blue region into 1.2 eV-photons ($\lambda = 1 \mu\text{m}$), would be an ideal phosphor for the c-Si cells.

In this study, we prepared oxyfluoride glass doped with Pr³⁺ and Yb³⁺ ions. Generally, glass material can be a preferred solution for solar cell applications, because it is transparent in wide wavelength regions, can be used as a cover material and thus can easily substitute for the conventional ones already used widely for the installed modules.

In this paper, the absorption, emission and excitation spectra of the glass were investigated. We examined energy transfer efficiency between Pr³⁺ and Yb³⁺ ions, particularly from Pr³⁺:³P₁ and ¹D₂ to the Yb³⁺-excited level by in-depth consideration of the emission spectra obtained. Comparing excitation spectra of Yb³⁺, emission and absorption spectra, as well as energy transfer efficiency, we obtain direct evidence of quantum cutting in the oxyfluoride glass.

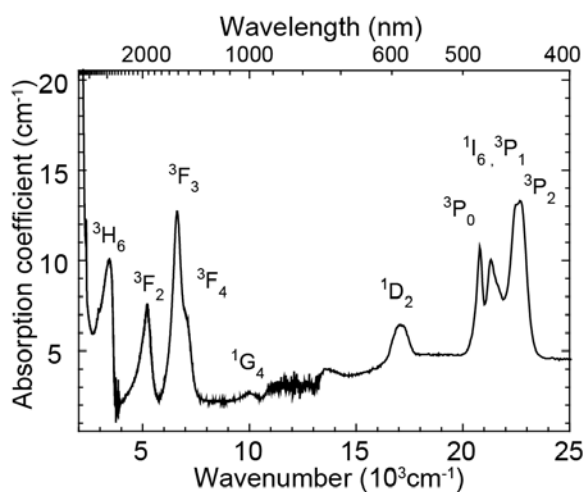
2. Experimental

A Pr³⁺-Yb³⁺ codoped glass with compositions of 32SrF₂-0.1PrF₃-2.9YbF₃-42SiO₂-23Al₂O₃ and Pr³⁺-Gd³⁺ codoped glass with compositions of 32SrF₂-xPrF₃-(3-x)GdF₃-42SiO₂-23Al₂O₃ (x = 0.1, 1) were prepared using SrF₂, PrF₃, YbF₃, GdF₃, SiO₂, Al₂O₃ as raw materials. Since the Gd³⁺ ion is optically inert in the wavelength range of visible to infrared, we will call the Pr³⁺-Gd³⁺ codoped glass as “Pr³⁺ singly doped glass”. All chemical powders had 99.9–99.99% purity. After mixing well in an alumina mortar, 20 g batches were melted in a platinum crucible at 1350 °C for 1.5 h. The melts were poured onto a stainless-steel plate at room-temperature and pressed by another plate. The obtained glass was annealed for 1 h at 500 °C below the glass transition temperature, which was determined by a differential scanning calorimeter, DSC (Rigaku, Thermo plus, DSC8270). The absorption spectrum was measured by using two kinds of absorption spectrometers (Shimadzu UV3600 and FT-IR8400S). The emission spectra in the range of 450–1200 nm were measured with a computer-controlled monochromator (Nikon, G-250) and a Si photodiode (Electro-Optical System Inc., S-025-H) by pumping with a 440 nm laser diode and a 590 nm light monochromatized by a bandpass filter (ASAHI SPECTRA, XBPA590) from a Xenon light source (ASAHI SPECTRA, MAX-302). Luminescence excitation spectrum was measured by using the Xenon light source, the monochromator and the Si photodiode with an 850 nm short-cut filter.

3. Results

Figure 1 shows the absorption spectrum of the glass doped with Pr^{3+} ions. The absorption bands of excited levels, $^3\text{H}_6$, $^3\text{F}_2$, $^3\text{F}_3$, $^3\text{F}_4$, $^1\text{G}_4$, $^1\text{D}_2$, $^3\text{P}_0$, $^3\text{P}_1$, $^1\text{I}_6$, $^3\text{P}_2$ were observed. Overlapping bands around 7000 cm^{-1} and $23,000\text{ cm}^{-1}$ were deconvoluted into two Gaussian bands by least-square fitting and the energy level values in the glass sample were determined. These absorption peak energy values were used to calculate the energy of Pr^{3+} emissions and to carry out the peak assignments. The Pr^{3+} singly doped glass has no strong absorption in the range of $500\text{ nm} \sim 1100\text{ nm}$ where c-Si solar cells have high conversion efficiency.

Figure 1. Absorption spectrum of the Pr^{3+} singly doped oxyfluoride glass ($x = 1.0$).



The emission spectra of the Pr^{3+} singly doped and the $\text{Pr}^{3+}\text{-Yb}^{3+}$ codoped samples excited at 440 nm and 590 nm light are shown in Figure 2 (a) and (b). The energy diagram of Pr^{3+} ion and transitions are shown in Figure 3. The emission spectrum of the Pr^{3+} singly doped sample excited at 590 nm showed 695 nm , 808 nm , 1030 nm emissions and these emissions originate from the $^1\text{D}_2 \rightarrow ^3\text{H}_5$, $^1\text{D}_2 \rightarrow ^3\text{F}_2$ and $^1\text{D}_2 \rightarrow ^3\text{F}_{3,4}$ transitions, respectively. In the emission spectrum of the Pr^{3+} singly doped sample excited at 440 nm , we observed several emissions from Pr^{3+} : $^3\text{P}_1$ and $^3\text{P}_0$ levels, 484 nm ($^3\text{P}_0 \rightarrow ^3\text{H}_4$), 520 nm ($^3\text{P}_1 \rightarrow ^3\text{H}_4$), 605 nm ($^3\text{P}_0 \rightarrow ^3\text{H}_6$), 642 nm ($^3\text{P}_0 \rightarrow ^3\text{F}_2$), 702 nm ($^3\text{P}_0 \rightarrow ^3\text{F}_3$), 722 nm ($^3\text{P}_0 \rightarrow ^3\text{F}_4$) and also observed emissions from the $^1\text{D}_2$.

The $\text{Pr}^{3+}\text{-Yb}^{3+}$ codoped sample showed Yb^{3+} ($^2\text{F}_{5/2} \rightarrow ^2\text{F}_{7/2}$) emission excited at both 440 nm and 590 nm . Under excitation at 440 nm , the intensity of the Yb^{3+} emission of the $\text{Pr}^{3+}\text{-Yb}^{3+}$ codoped sample was about twice as large as the Pr^{3+} emissions. We also found that the Pr^{3+} emission peak around 600 nm of the $\text{Pr}^{3+}\text{-Yb}^{3+}$ codoped sample is quite different from that of the singly doped one. Under excitation at 590 nm , we cannot observe Pr^{3+} emissions in the $\text{Pr}^{3+}\text{-Yb}^{3+}$ codoped sample.

Figure 4 shows the excitation spectrum of Yb^{3+} $1\mu\text{m}$ luminescence of the $\text{Pr}^{3+}\text{-Yb}^{3+}$ codoped glass and the absorption spectrum of the Pr^{3+} singly doped glass. The excitation cross-section ratio of the $^1\text{D}_2$ to the $^3\text{P}_1$ band was approximately 1:10 and the absorption cross-section ratio was approximately 1:6.

Figure 2. Emission spectra of the Pr³⁺ singly doped and Pr³⁺-Yb³⁺ codoped samples excited at (a) 590 nm and (b) 440 nm.

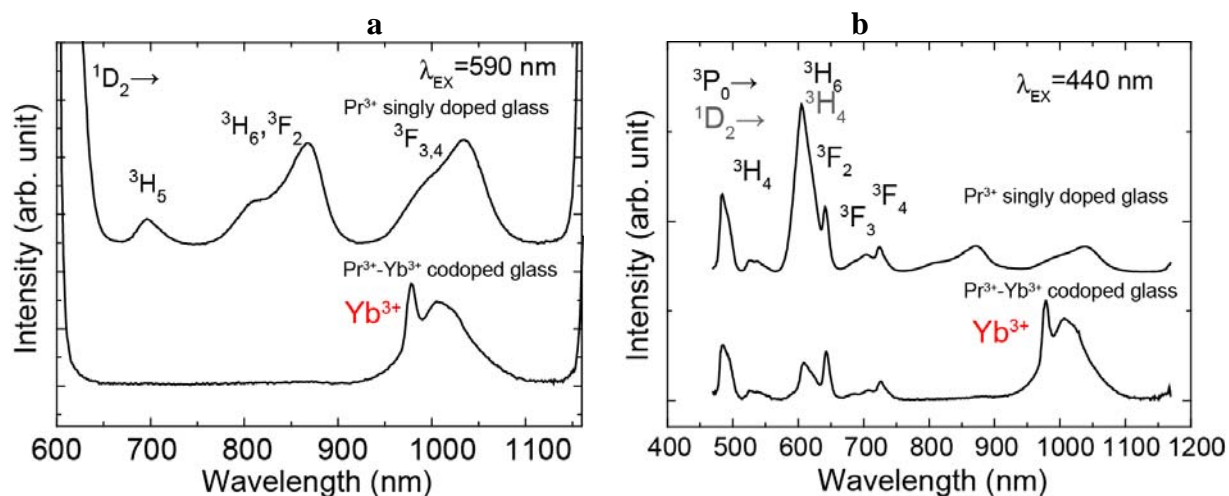


Figure 3. Energy level diagram of Pr³⁺ with transitions excited at (a) 590 nm and (b) 440 nm.

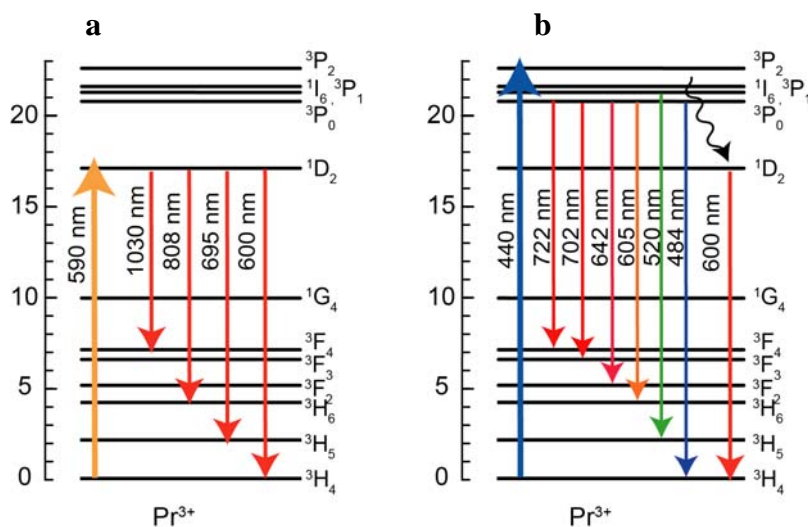
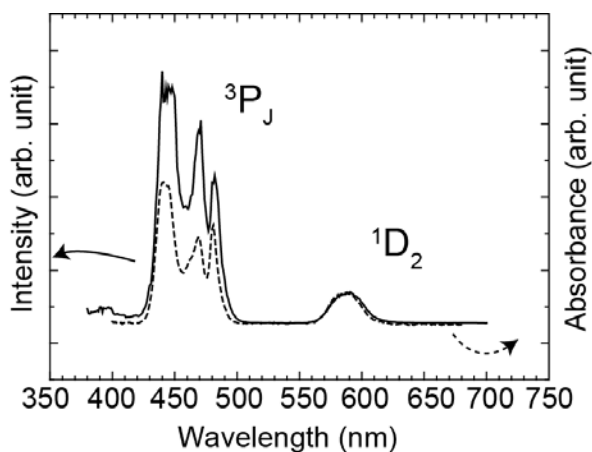


Figure 4. Excitation spectrum of Yb³⁺ 1μm luminescence of the Pr³⁺-Yb³⁺ codoped glass (solid line) and absorption spectrum of the Pr³⁺ doped glass (dotted line).



4. Discussion

In the codoped sample, the Pr^{3+} concentration is so low (0.1 mol %) that cross relaxation and energy migration processes between Pr^{3+} ions can be neglected. As indicated in Figure 2 (b), the Pr^{3+} singly doped glass showed the $\text{Pr}^{3+}:^1\text{D}_2$ emissions. This indicates that multi-phonon relaxation from $^3\text{P}_0$ to $^1\text{D}_2$ occurs in the sample. Taking into account the multi-phonon relaxation from $^3\text{P}_0$ to $^1\text{D}_2$, we find that the emission band around 600 nm is a convolution of two bands, due to transitions of $^3\text{P}_0 \rightarrow ^3\text{H}_6$ and $^1\text{D}_2 \rightarrow ^3\text{H}_4$.

Yb^{3+} emissions were observed in the $\text{Pr}^{3+}\text{-Yb}^{3+}$ codoped glass excited at both 440 nm and 590 nm. This result indicates two energy transfers (ET) from Pr^{3+} to Yb^{3+} ions: $(\text{Pr}^{3+}:^3\text{P}_0 \rightarrow ^1\text{G}_4) \rightarrow (\text{Yb}^{3+}:^2\text{F}_{5/2} \leftarrow ^2\text{F}_{7/2})$ and $(\text{Pr}^{3+}:^1\text{D}_2 \rightarrow ^3\text{F}_4, ^3\text{F}_3) \rightarrow (\text{Yb}^{3+}:^2\text{F}_{5/2} \leftarrow ^2\text{F}_{7/2})$, as shown in Figure 5.

Now, we discuss ET efficiency (η_{ET}) from Pr^{3+} to Yb^{3+} ions in the $\text{Pr}^{3+}\text{-Yb}^{3+}$ codoped sample. ET efficiency (η_{ET}) can be expressed by the following equation (1),

$$\eta_{\text{ET}} = \frac{W_{\text{ET}}}{A + W_{\text{MP}} + W_{\text{ET}}} \quad (1)$$

where A is radiative transition, W_{MP} is multi-phonon relaxation and W_{ET} represents ET rate. Since the radiative transitions from $\text{Pr}^{3+}:^3\text{P}_0$ level were observed as indicated in Figure 2 (b), ET efficiency from $\text{Pr}^{3+}:^3\text{P}_0$ to Yb^{3+} , $\eta_{\text{ET}}(^3\text{P}_0)$ is less than 100%. On the other hand, as indicated in Figure 2 (a), no radiative transition of $\text{Pr}^{3+}:^1\text{D}_2$ was observed. Since almost all of $^1\text{D}_2$ emissions were quenched, ET efficiency from $\text{Pr}^{3+}:^1\text{D}_2$ to Yb^{3+} , $\eta_{\text{ET}}(^1\text{D}_2)$ is close to 100%. Therefore, the $\eta_{\text{ET}}(^1\text{D}_2)$ is higher than the $\eta_{\text{ET}}(^3\text{P}_0)$. The radiative transition, A , for $^3\text{P}_0$ is very likely to be higher than for $^1\text{D}_2$, as the radiative lifetime of the former level is usually shorter than for the latter. This is one reason why the $\eta_{\text{ET}}(^1\text{D}_2)$ is higher than the $\eta_{\text{ET}}(^3\text{P}_0)$. It is likely that in the present system $W_{\text{MP}}(^1\text{D}_2)$ is negligible, due to the relatively large energy gap, and for $^1\text{D}_2$ W_{ET} is larger than A ; this makes $\eta_{\text{ET}}(^1\text{D}_2)$ close to 100%. For $^3\text{P}_0$, W_{MP} is more important due to the smaller gap, and also A is higher, making $\eta_{\text{ET}}(^3\text{P}_0)$ less than 100%.

Excitation spectrum monitoring the Yb^{3+} emission and the absorption spectrum are shown in Figure 4. Area ratio of the $^1\text{D}_2$ band to the $^3\text{P}_J$ band in the excitation spectrum was 1:10, while that of the absorption spectrum was 1:6. When we assume that excitation efficiency to Yb^{3+} from $^3\text{P}_J$ and that from $^1\text{D}_2$ are equivalent, the emission intensity of Yb^{3+} ions by excited $^3\text{P}_J$ levels is more than 1.6 times as strong as that of the $^1\text{D}_2$ level. In fact, there is the following relation between the $^3\text{P}_J$ band and the $^1\text{D}_2$ band: $\text{EX}(^3\text{P}_J)/\text{EX}(^1\text{D}_2) > 1.6$, where $\text{EX}(^3\text{P}_J)$ and $\text{EX}(^1\text{D}_2)$ are the excitation efficiency of $^3\text{P}_J$ and $^1\text{D}_2$, respectively. This is direct evidence of quantum cutting as indicated in Figure 6. In the case of the ET processes shown in Figure 5, ETs from both $^1\text{D}_2$ and $^3\text{P}_0$ of Pr^{3+} to Yb^{3+} are one photon to one photon processes. As previously mentioned, the ET efficiency from $^1\text{D}_2$ ($\eta_{\text{ET}}(^1\text{D}_2)$) is higher than that from $^3\text{P}_0$ ($\eta_{\text{ET}}(^3\text{P}_0)$). If the ET occurs as shown in Figure 5, the excitation efficiency ratio of Yb^{3+} , $\text{EX}(^3\text{P}_J)/\text{EX}(^1\text{D}_2)$ is less than unity. Thus, the one photon-one photon ET process cannot explain the experimental results. There is the possibility of a cooperative three body energy transfer between one excited Pr^{3+} and two Yb^{3+} ions, as shown in Figure 6. The ideal one photon to two photon process, $\text{EX}(^3\text{P}_J)/\text{EX}(^1\text{D}_2) = 2$ can be achieved in the case of low nonradiative loss due to slow multi-phonon relaxation from $^3\text{P}_0$ and $^1\text{G}_4$.

Figure 5. Energy transfer mechanisms of Pr^{3+} and Yb^{3+} excited at (a) 590 nm and (b) 440 nm.

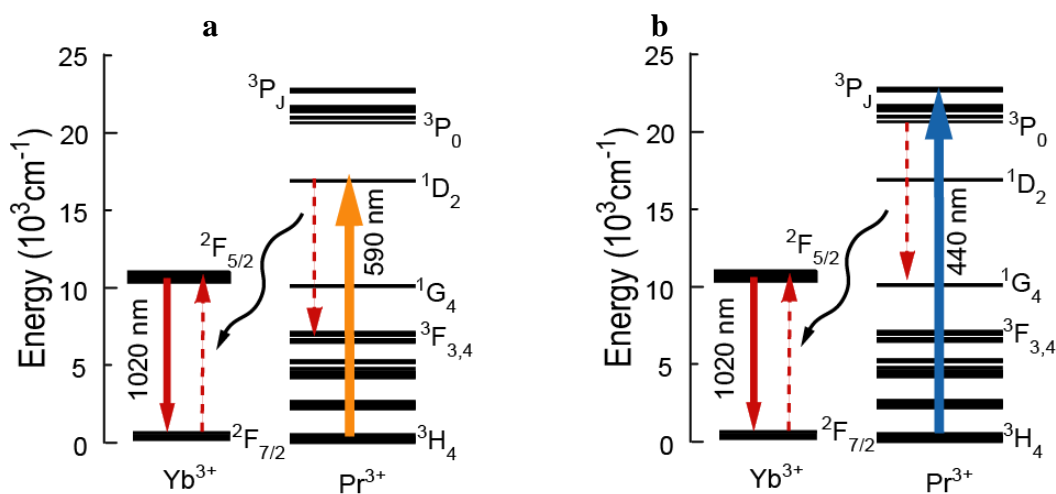
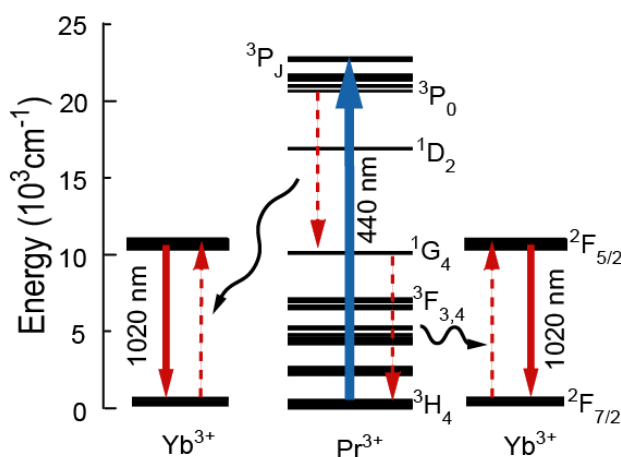


Figure 6. Schematic diagram of quantum cutting between Pr^{3+} and Yb^{3+} ions.



5. Conclusions

The Pr^{3+} - Yb^{3+} codoped oxyfluoride glass showed Yb^{3+} emissions when excited at Pr^{3+} : $^3\text{P}_J$ and $^1\text{D}_2$ indicating two schemes of ET: (Pr^{3+} : $^3\text{P}_0 \rightarrow ^1\text{G}_4$) \rightarrow (Yb^{3+} : $^2\text{F}_{5/2} \leftarrow ^2\text{F}_{7/2}$) and (Pr^{3+} : $^1\text{D}_2 \rightarrow ^3\text{F}_4$, $^3\text{F}_3$) \rightarrow (Yb^{3+} : $^2\text{F}_{5/2} \leftarrow ^2\text{F}_{7/2}$). Comparing the Yb^{3+} excitation spectrum to the absorption spectrum, we find that the Yb^{3+} excitation efficiency by $^3\text{P}_J$, $\text{EX}(^3\text{P}_J)$ is 1.6 times greater than $\text{EX}(^1\text{D}_2)$, which indicates that two step ETs of (Pr^{3+} : $^3\text{P}_0 \rightarrow ^1\text{G}_4$) \rightarrow (Yb^{3+} : $^2\text{F}_{5/2} \leftarrow ^2\text{F}_{7/2}$) and ET(Pr^{3+} : $^1\text{G}_4 \rightarrow ^3\text{H}_4$) \rightarrow (Yb^{3+} : $^2\text{F}_{5/2} \leftarrow ^2\text{F}_{7/2}$) occur in the Pr^{3+} - Yb^{3+} codoped glass when excited at 440 nm. This is the direct evidence of quantum cutting. The direct evidence of quantum cutting in a glass sample supports its promising application to improve the solar cell efficiency.

References and Notes

1. Sommerdijk, J.L.; Bril, A.; de Jager, A.W. Two photon luminescence with ultraviolet excitation of trivalent praseodymium. *J. Lumin.* **1974**, *8*, 341–343.

2. Piper, W.W.; DeLuca, J.A.; Ham, F.S. Cascade fluorescent decay in Pr³⁺-doped fluorides: Achievement of a quantum yield greater than unity for emission of visible light. *J. Lumin.* **1974**, *8*, 344–348.
3. Wegh, R.T.; Donker, H.; Meijerink, A.; Lamminmäki, R.J.; Hölsä, J. Vacuum-ultraviolet spectroscopy and quantum cutting for Gd³⁺ in LiYF₄. *Phys. Rev. B.* **1997**, *56*, 13841–13848.
4. Wegh, R.T.; Donker, H.; Oskam, K.D.; Meijerink, A. Visible quantum cutting in LiGdF₄:Eu³⁺ through downconversion. *Science* **1999**, *283*, 663–666.
5. B.M.; van der Ende, L.; Aarts, A. Meijerink. Near-Infrared Quantum Cutting for Photovoltaics. *Adv. Mater.* **2009**, *21*, 3073–3077.
6. Vergeer, P.; Vlugt, T.J.H.; Kox, M.H.F.; den Hertog, M.I.; van der Eerden, J.P.J.M.; Meijerink, A. Quantum cutting by cooperative energy transfer in Yb_xY_{1-x}PO₄ : Tb³⁺. *Phys. Rev. B* **2005**, *71*, 014119.
7. Song, Y.; Bin, Z.; Jingxin, C.; Jin, L.; Jian Rong, Q. Infrared quantum cutting in Tb³⁺, Yb³⁺ codoped transparent glass ceramics containing CaF₂ nanocrystals. *Appl. Phys. Lett.* **2008**, *92*, 141112.
8. Zhang, Q.Y.; Yang, G.F.; Jiang, Z.H. Cooperative downconversion in GdAl₃(BO₃)₄:RE³⁺, Yb³⁺ (RE = Pr, Tb, and Tm). *Appl. Phys. Lett.* **2007**, *91*, doi: 10.1063/1.2757595.
9. Richards, B.S. Luminescent layers for enhanced silicon solar cell performance: Down-conversion. *Sol. Energy Mater. Sol. Cells* **2006**, *90*, 1189–1207.
10. Strümpel, C.; McCann, M.; Beaucarne, G.; Arkhipov, V.; Slaoui, A.; Švrček, V.; del Cañizo, C.; Tobias, I. Modifying the solar spectrum to enhance silicon solar cell efficiency-An overview of available materials. *Sol. Energy Mater. Sol. Cells* **2007**, *91*, 238–249.
11. Trupke, T.; Green, M.A.; Wurfel, P. Improving solar cell efficiencies by down-conversion of high-energy photons. *J. Appl. Phys.* **2002**, *92*, 1668–1674.
12. William, S.; Hans, J.Q. Detailed Balance Limit of Efficiency of p-n Junction Solar Cells. *J. Appl. Phys.* **1961**, *32*, 510–519.

© 2010 by the authors; licensee Molecular Diversity Preservation International, Basel, Switzerland. This article is an open-access article distributed under the terms and conditions of the Creative Commons Attribution license (<http://creativecommons.org/licenses/by/3.0/>).